

MCCULLOUGH, S.D., GELDENHUYS, I.J. and JONES, R.T. Pyrometallurgical iron removal from a PGM-containing alloy. *Third International Platinum Conference 'Platinum in Transformation'*, The Southern African Institute of Mining and Metallurgy, 2008.

Pyrometallurgical iron removal from a PGM-containing alloy

S.D. MCCULLOUGH, I.J. GELDENHUYS, and R.T. JONES

Mintek

Iron-based alloys are very good collectors of platinum group metals (PGMs) and base metals. A number of smelting processes have been developed in recent years that produce iron-rich alloys. As a precursor to base metals removal and precious metals refining, it is necessary to remove iron from the alloy. This can be done either hydrometallurgically or pyrometallurgically. This paper discusses the pyrometallurgical option for iron removal (by blowing the molten alloy with either air or oxygen). Results are presented from a range of tests on a PGM-containing alloy, such as is produced in the ConRoast process.

Introduction

Mintek's ConRoast process recovers platinum group metals (PGMs) from roasted or low S-bearing concentrates in an iron-rich alloy (typically 70 to 85% Fe) during mild reductive smelting. Any subsequent processing of this alloy will inevitably require some form of iron removal to upgrade the valuable base and precious metal concentrations in the alloy. The iron removal step can be accomplished by either hydrometallurgical or pyrometallurgical means. This work focuses on the pyrometallurgical removal of iron in the molten state through oxidation.

Pyrometallurgical iron removal, to upgrade base and precious metal concentrations through oxidation, is typically accomplished via gas injection into the molten bath. This process is more commonly known as converting. While the South African PGM industry typically removes Fe from sulphide-rich liquids (matte), in this case the process involves Fe removal from an iron-rich ConRoast alloy that is deficient in sulphur. This study examines, at the laboratory scale, the converting behaviour of an iron-rich alloy that was produced from the smelting of high-Cr low-S revert tailings in Mintek's 1.5 MW DC arc furnace.

Experimental work

Alloy charges were contained in high-purity sintered alumina crucibles and melted using induction heating. Oxygen was introduced to the melt using an alumina tube which was continuously lowered throughout the test to ensure it was immersed in the alloy as either the tube was consumed or the alloy level decreased. The rate and quantity of oxygen delivered was controlled using mass flow controllers or rotameters. The temperature of the melt was frequently measured using an optical pyrometer. Additions of CaO, SiO₂, and Al₂O₃ were made periodically to flux the Fe-rich slag that formed. The use of both CaO and SiO₂ ensured a low-melting slag, whilst Al₂O₃ was added to ensure protection of the alumina crucibles.

Approximately 0.7 to 1 kg of alloy was used, although several larger-scale tests (approximately 5 kg) were also conducted. These larger-scale tests were primarily aimed at

generating sufficient converted alloy for further hydrometallurgical testwork.

To achieve higher degrees of Fe removal and maintain a sufficiently large alloy pool at the late stages of converting, it was sometimes necessary to conduct the converting in two stages (Tests 5, 6, and 7) due to the large slag volumes generated and crucible volume limitations. In the case of Tests 5 and 6, a larger than normal amount of alloy was converted to approximately 60 to 70% Fe-removal in the first stage. The tests were terminated at this stage and allowed to cool whereupon the alloy was separated from the slag, placed in a new crucible, brought to the desired temperature and converted further. In the case of Test 7, two lots of alloy were converted to similar levels of Fe-removal (Tests 7.1 and 7.2), and were combined and converted further in Test 7.3.

Generally, the converting process was characterized by mild turbulence of the bath, owing to the stirring effect of the oxygen. Gas was not evolved from the bath for much of the converting, thereby indicating efficient reaction between the alloy and gas. With the exception of Test 8, little fume or volatiles were observed and only a faint odour of SO₂ was detected for much of the converting test. The flux additions for Tests 1 to 7 made use of CaO, and were distinctly different from Test 8 in this regard. Given the high degree of partitioning of S to the slag that was observed for the previous tests, Test 8 made use of a CaO-free flux to examine the effect of slag composition on the degree of S removal from the alloy. In this test, copious amounts of SO₂ were evolved from the melt particularly towards the end of the test. On the whole, the flux additions and high Fe concentration in the slag resulted in a molten slag that generally had a low viscosity. Experimental details are given in Table I.

Results

The composition of the starting alloy is shown in Table II, and individual PGM concentrations are shown in Table III. The composition was determined from alloy samples taken from the molten alloy at the start of each of the converting tests, using a silica sampling tube.

Table I
Experimental details for the converting test

| Test | Inputs | | Products | | | Flux Additions | | |
|------|---------------------------------|---------------------|--------------------------|---------------------------|-------------------------------------|--|-------------------------|--------------------------------------|
| | O ₂ supplied* (%) | Alloy start (g) | Slag [§] (%) | Alloy [§] (%) | Alloy mass loss [§] (%) | Al ₂ O ₃ [§] (%) | CaO [§] (%) | SiO ₂ [§] (%) |
| 1 | 29.0 | 664.1 | 72.5 | 61.6 | 38.4 | 4.7 | 3.9 | 2.4 |
| 2 | 62.8 | 622.0 | 117.1 | 31.7 | 68.3 | 10.5 | 8.0 | |
| 3 | 72.8 | 620.6 | 125.4 | 29.6 | 70.4 | 10.5 | 10.5 | |
| 4 | 83.9 | 621.3 | 152.3 | 17.9 | 82.1 | 14.5 | 14.5 | 7.2 |
| 5.1 | 58.4 | 913.8 | 77.4 [@] | 43.9 | 56.1 | 9.3 | 7.1 | 3.3 |
| 5.2 | 90.1 [#] | 376.0 | 145.6 | 20.0 | 80.0 (91.3) [†] | 16.0 | 16.0 | 16.0 |
| 6.1 | 64.9 | 884.6 | 118.5 | 37.4 | 62.6 | 6.8 | 6.8 | 6.8 |
| 6.2 | 88.6 [#] | 300.0 | 145.8 | 23.1 | 76.9 (91.9) [†] | 20.0 | 20.0 | 20.0 |
| 7.1 | 63.9 | 5130.2 | 115.2 | 25.8 | 74.2 | 7.8 | 5.8 | 5.8 |
| 7.2 | 67.6 | 5130.3 | 108.5 | 21.0 | 79.0 | 7.8 | 5.8 | 5.8 |
| 7.3 | 91.4 [#] | 2366.9 [§] | 127.3 | 36.6 | 63.4 (90.4) [†] | 16.9 | 12.7 | 16.9 |
| 8 | 84.6 | 5021.9 | 128.1 | 11.2 | 88.8 | 11.5 | - | 17.1 |

* Quantity of oxygen supplied expressed as a percentage of the total amount of oxygen required to oxidize all the Fe, Cr, and Si contained in the alloy to FeO, Cr₂O₃, and SiO₂ (this equates to 22.5 g of oxygen per 100 g of alloy)

§ Masses expressed as a percentage of the starting alloy mass

Cumulative oxygen amount delivered over both stages of the test

† Figures in parentheses represent the cumulative alloy mass loss for the combined stages of converting.

@ Test suffered from crucible failure and slag was lost from the crucible.

§ Combined alloy from Tests 7.1 and 7.2 less sample masses

Table II
Chemical composition of the starting alloy (mass %)

| | Si | Cr | Fe | Co | Ni | Cu | S | ΣPGM | Total |
|----------------|------|------|------|------|------|------|------|--------|-------|
| Mean | 0.25 | 0.08 | 77.4 | 1.04 | 8.49 | 3.21 | 5.46 | 0.0641 | 96.0 |
| Std. Deviation | 0.21 | 0.04 | 2.09 | 0.13 | 0.49 | 0.29 | 1.63 | 0.0034 | |

ΣPGM = Pt + Pd + Rh + Ru + Ir + Au as determined by fire assay Ni-sulphide collection

Table III
Individual PGM concentrations of the starting alloy (mass %)

| | Pt | Pd | Rh | Ru | Ir | Au | Total |
|----------------|--------|--------|--------|--------|--------|--------|--------|
| Mean | 0.0335 | 0.0150 | 0.0052 | 0.0084 | 0.0015 | 0.0006 | 0.0641 |
| Std. Deviation | 0.0026 | 0.0012 | 0.0004 | 0.0006 | 0.0002 | 0.0001 | 0.0034 |

During heating, the alloys were found to melt between 1 250 and 1 350°C, and, once molten, the energy supplied by the induction furnace was maintained at the level required to keep the alloy in the molten state. During converting of the smaller-scale tests (0.7 kg), the temperature of the melt rose to typically 1 400°C without adjustment to the power input, indicating the exothermic nature of the conversion process. With the larger-scale tests (5 kg), at the full rate of oxygen delivery, the slag frequently attained a temperature of between 1 440 and 1 520°C, and the external heating of the melt was terminated to prevent further increases in temperature.

The resulting alloy and slag compositions are shown in Table IV and Table V.

Discussion

Alloy composition during converting: base and precious metals

With the addition of oxygen to the alloy, different elements will be oxidized to different extents, depending on the relative stabilities of their oxides. Hence, Si will be largely removed from the alloy before Ni, for example. The

question addressed in this study is how the removal of these elements affects the alloy composition. The primary oxidation reaction affecting the alloy composition is that of Fe. The relationship between the amount of oxygen delivered (expressed as a percentage of the total required for complete Fe, Cr, and Si removal) and the degree of Fe removal is shown in Figure 1. The degree of Fe removal is defined as (mass of Fe in starting alloy – mass of Fe in final alloy)/(mass of Fe in starting alloy), expressed as a percentage. The alloy exhibits a relatively linear degree of Fe removal with oxygen delivery. This indicates that the overall degree of Fe removal is proportional to the amount of oxygen delivered, and that oxygen efficiency is high. It appears that converting, under the conditions tested, is not limited by kinetic or mass transfer considerations.

Alloy mass loss was also found to be linearly dependent on the degree of Fe removal (Figure 2) for the range of conditions tested. While this relationship is not surprising in light of the high oxygen efficiencies, it indicates that the converting reaction is dominated by Fe removal from the alloy even at higher degrees of Fe removal.

As converting proceeds, the concentration of Fe in the alloy initially (up to approximately 70% Fe removal)

Table IV
Chemical composition of the alloys (mass%)

| Test | Fe | Co | Ni | Cu | S | Pt | Pd | Rh | Ru | Ir | Au | ΣPGM | Total |
|------|------|------|------|------|------|--------|--------|--------|--------|--------|--------|--------|-------|
| 1 | 71.0 | 1.64 | 12.4 | 3.95 | 3.80 | 0.0583 | 0.0219 | 0.0070 | 0.0115 | 0.0023 | 0.0009 | 0.1018 | 93.3 |
| 2 | 59.5 | 2.99 | 24.1 | 6.82 | 2.47 | 0.1001 | 0.0446 | 0.0150 | 0.0252 | 0.0049 | 0.0020 | 0.1916 | 96.3 |
| 3 | 53.9 | 3.19 | 27.6 | 7.57 | 2.63 | 0.1090 | 0.0499 | 0.0171 | 0.0281 | 0.0054 | 0.0022 | 0.2115 | 95.3 |
| 4 | 34.6 | 3.67 | 35.9 | 9.63 | 4.78 | 0.1825 | 0.0704 | 0.0257 | 0.0378 | 0.0075 | 0.0032 | 0.3271 | 89.4 |
| 5.1 | 64.7 | 2.34 | 19.3 | 5.77 | 3.06 | 0.0744 | 0.0344 | 0.0115 | 0.0191 | 0.0034 | 0.0015 | 0.1441 | 95.5 |
| 5.2 | 4.26 | 0.78 | 65.2 | 17.7 | 9.97 | 0.3390 | 0.1490 | 0.0516 | 0.0858 | 0.0155 | 0.0071 | 0.6479 | 99.4 |
| 6.1 | 59.7 | 2.60 | 22.1 | 6.30 | 3.71 | 0.0869 | 0.0400 | 0.0136 | 0.0226 | 0.0041 | 0.0018 | 0.1688 | 94.9 |
| 6.2 | 3.42 | 0.95 | 66.9 | 15.5 | 9.44 | 0.3125 | 0.1390 | 0.0476 | 0.0774 | 0.0161 | 0.0064 | 0.5989 | 97.6 |
| 7.1 | 47.8 | 2.87 | 35.1 | 8.20 | 2.67 | 0.1350 | 0.0669 | 0.0231 | 0.0367 | 0.0040 | 0.0029 | 0.2686 | 97.2 |
| 7.2 | 30.5 | 3.82 | 41.7 | 12.5 | 5.20 | 0.1525 | 0.0795 | 0.0256 | 0.0411 | 0.0062 | 0.0036 | 0.3084 | 96.4 |
| 7.3 | 8.04 | 2.52 | 68.6 | 14.3 | 6.39 | 0.2700 | 0.1240 | 0.0447 | 0.0741 | 0.0087 | 0.0054 | 0.5270 | 101.9 |
| 8 | 12.4 | 1.99 | 49.7 | 18.2 | 19.9 | 0.2809 | 0.1258 | 0.0429 | 0.0698 | 0.0120 | 0.0055 | 0.5370 | 103.4 |

NB Si and Cr <0.05%

ΣPGM = Pt + Pd + Rh + Ru + Ir + Au as determined by fire assay Ni-sulphide collection

Table V
Chemical compositions of the slags (mass %)

| Test | MgO | Al ₂ O ₃ | SiO ₂ | CaO | Cr ₂ O ₃ | FeO | CoO | NiO | CuO | S | ΣPGM | Total |
|------|------|--------------------------------|------------------|------|--------------------------------|------|------|------|------|------|--------|-------|
| 1 | 0.64 | 6.96 | 3.91 | 4.69 | 0.61 | 77.3 | 0.06 | 0.46 | 1.93 | 7.42 | 0.0007 | 104.0 |
| 2 | 0.61 | 13.2 | 0.45 | 6.35 | 0.25 | 72.8 | 0.07 | 0.60 | 1.45 | 4.48 | 0.0007 | 100.3 |
| 3 | 0.25 | 10.4 | 0.43 | 8.77 | <0.05 | 72.6 | 0.08 | 0.36 | 1.46 | 4.78 | 0.0004 | 99.2 |
| 4 | 0.50 | 12.7 | 5.58 | 7.86 | 0.14 | 67.0 | 0.15 | 0.51 | 1.20 | 3.34 | 0.0004 | 99.1 |
| 5.1 | 0.53 | 12.6 | 3.17 | 5.53 | 0.22 | 76.9 | 0.03 | 0.39 | 1.21 | 4.26 | 0.0003 | 104.9 |
| 5.2 | 0.20 | 18.0 | 10.0 | 9.43 | <0.05 | 50.4 | 1.64 | 4.14 | 1.21 | 0.42 | 0.0007 | 95.5 |
| 6.1 | 0.45 | 9.85 | 6.10 | 4.88 | 0.22 | 69.2 | 0.03 | 0.37 | 1.44 | 3.93 | 0.0004 | 96.5 |
| 6.2 | 0.18 | 19.0 | 12.6 | 11.5 | <0.05 | 48.2 | 1.70 | 3.76 | 1.08 | 0.41 | 0.0004 | 98.5 |
| 7.1 | 0.55 | 7.57 | 5.55 | 4.66 | 0.35 | 73.0 | 0.27 | 0.67 | 1.33 | 4.42 | 0.0012 | 98.4 |
| 7.2 | 0.47 | 8.81 | 5.26 | 4.59 | 0.30 | 72.4 | 0.33 | 0.77 | 1.31 | 4.09 | 0.0011 | 98.3 |
| 7.3 | 0.13 | 12.8 | 11.8 | 8.86 | <0.05 | 50.1 | 2.73 | 4.84 | 1.19 | 0.36 | 0.0114 | 92.9 |
| 8 | 0.49 | 11.0 | 12.1 | 0.08 | 0.29 | 64.6 | 0.69 | 1.60 | 1.64 | 2.00 | 0.0012 | 94.5 |

NB TiO₂, V₂O₅, MnO, Pb, and Zn <0.05%

ΣPGM = total PGM as determined by fire assay Pb collection (i.e. Pt, Pd, Rh, and Au)

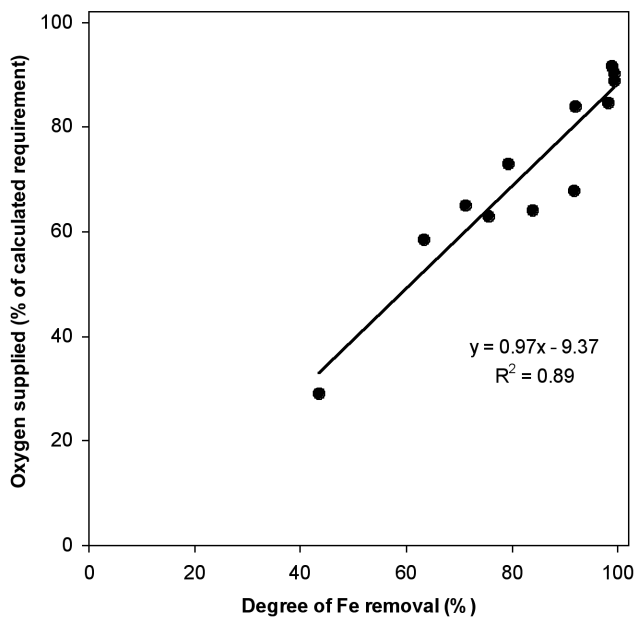


Figure 1. Comparison of the amount of oxygen supplied and the degree of Fe removal

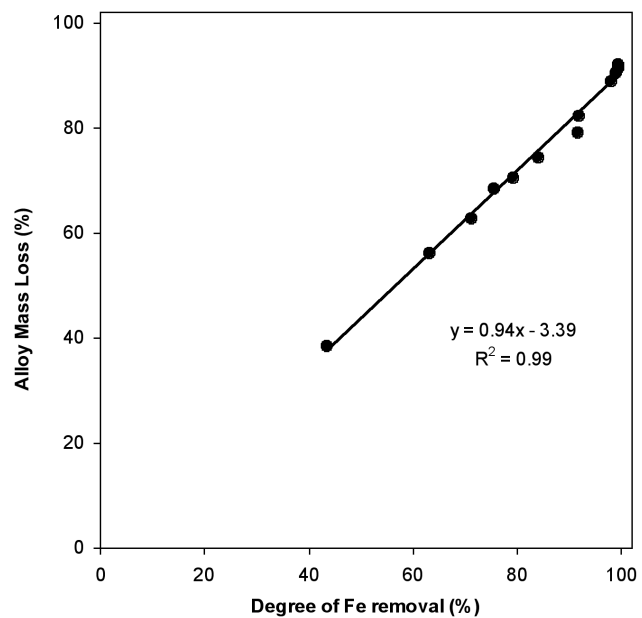


Figure 2. Comparison of the loss in alloy mass with the degree of Fe removal

$$\text{Degree of Fe removal} = \left(1 - \frac{\text{Mass Fe in final alloy}}{\text{Mass Fe in start alloy}}\right) \times 100\%$$

decreases relatively slowly (Figure 3). However, as converting passes this position, the Fe concentration decreases more rapidly. Two important points can be gathered from this observation:

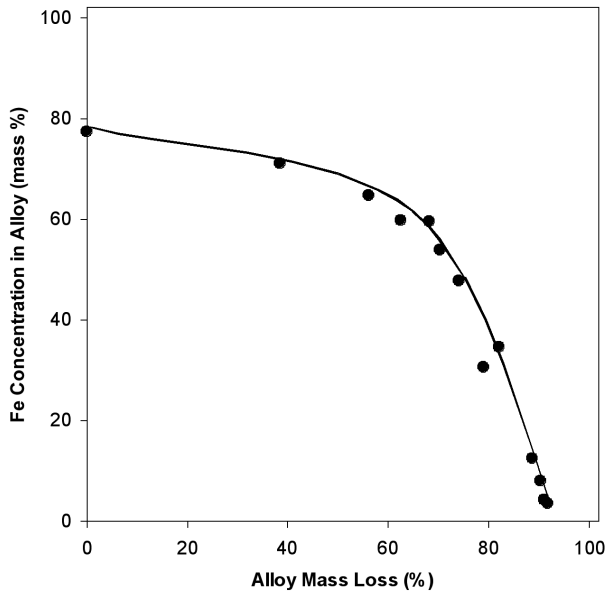


Figure 3. Concentration of Fe in alloy as a function of alloy mass loss

- An alloy that has lost 70% of its mass during converting can still contain significant concentrations of Fe (55%).
- At higher levels of conversion, the decrease in Fe concentration is rapid for relatively small increases in the amount of oxygen delivered.

As Fe is removed from the alloy, more noble elements tend to be concentrated in the alloy, as seen from the increase in concentrations of Ni, Cu (Figure 4) and PGMs (Figure 5). As higher levels of Fe removal are achieved, the rate of increase in the concentration of Ni, Cu, and PGMs increases. Co, on the other hand, displays a minor increase in concentration followed by a marked decrease as high levels of conversion are obtained; this is because of the increasing amount of Co oxidation that takes place as the extent of conversion increases.

Recovery to the alloy during converting: base and precious metals

When oxygen is added to the molten alloy, the various metallic elements oxidize to different extents, at a given level of oxygen delivery. This behaviour allows for a reasonable degree of Fe removal to take place during converting without significant losses of the pay-metals to the slag. The interchange between Co and Fe, for example, can be seen by studying the liquid reaction between slag and alloy:



At equilibrium, the degree of separation between Co and Fe can be indicated by the equilibrium constant, *K*, which is strictly a function of temperature. Over the temperature range of interest, *K* for Equation [1] has a value of approximately 30. The activities *a* may be expressed in terms of activity coefficients γ and mole fractions *x*.

$$K = \frac{a_{\text{Co}} \cdot a_{\text{FeO}}}{a_{\text{CoO}} \cdot a_{\text{Fe}}} = \frac{\gamma_{\text{Co}} x_{\text{Co}} \cdot \gamma_{\text{FeO}} x_{\text{FeO}}}{\gamma_{\text{CoO}} x_{\text{CoO}} \cdot \gamma_{\text{Fe}} x_{\text{Fe}}} \quad [2]$$

While individual activity coefficients may be obtained from the literature, in the interests of simplicity, we may combine

the ratio of the activity coefficients of these four chemical species in solution.

$$\gamma = \frac{\gamma_{\text{CoO}} \cdot \gamma_{\text{Fe}}}{\gamma_{\text{Co}} \cdot \gamma_{\text{FeO}}} \quad [3]$$

If we make the reasonable assumption that γ for Co is not a strong function of composition, then we may derive a simple expression to show the relationship between the recovery of Co to the alloy and the recovery of Fe to the alloy. Therefore from Equations [2] and [3], *K* γ for Co may be expressed as:

$$K\gamma = \frac{x_{\text{Co}} \cdot x_{\text{FeO}}}{x_{\text{CoO}} \cdot x_{\text{Fe}}} \quad [4]$$

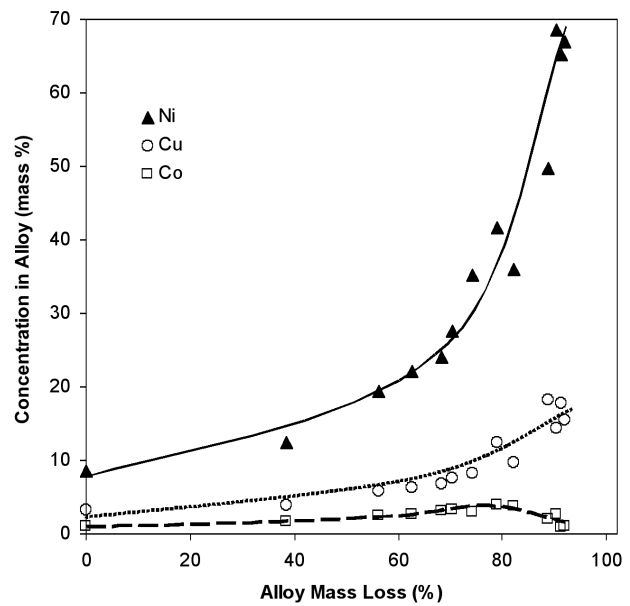


Figure 4. Concentration of Ni, Cu, and Co in the alloy as a function of alloy mass loss

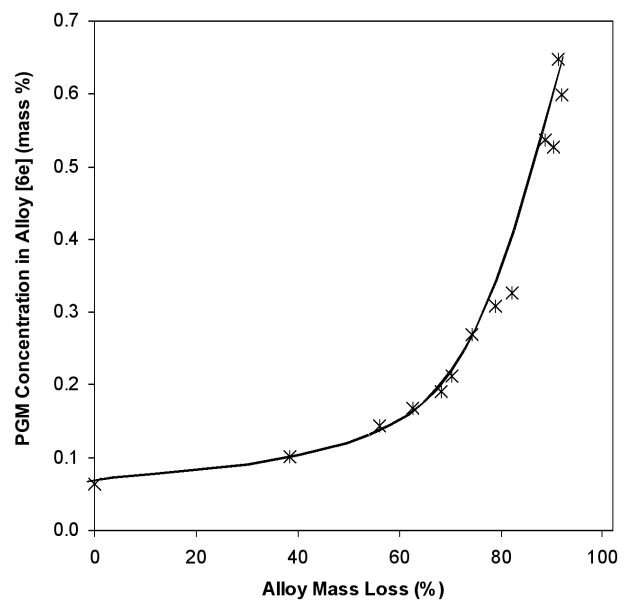


Figure 5. Concentration of PGMs (6e) in alloy as a function of alloy mass loss

Utilizing mass balance principles¹, the characteristic relationship between Fe recovery and Co recovery to the alloy phase may then be expressed as:

$$R_{Co} = \frac{K\gamma \cdot R_{Fe}}{1 - (1 - K\gamma)R_{Fe}} \quad [5]$$

It is possible to calculate a value for $K\gamma$ from published theoretical data, but this would apply strictly to a perfect equilibrium system. Values of $K\gamma$ may therefore also be found by fitting Equation [5] to experimental data. As explained above for the interchange between Co and Fe, the same principle was applied to develop the recovery correlation for Ni². The functional relationship expressed in Equation [5] provides a valuable tool through which the experimental $K\gamma$ values for the various elements can be evaluated. This equation was originally developed for the context of reductive smelting, but is equally applicable to converting.

The experimental data for the various converting tests is depicted as department of the pay-metal versus the degree of Fe removal. Excellent correlations were found for Ni (Figure 6) and Co (Figure 7) with $K\gamma$ values of 100 and 31 respectively. From the shape of the curves, it is clear that increased $K\gamma$ values represent conditions with decreased losses of the pay-metals to the slag phase. It may also be possible to optimize these conditions or effectively maximize the $K\gamma$ values by modifying the slag compositions (because activity coefficients are a function of composition as well as temperature). The mechanism through which PGM department is defined was not evaluated as part of this study, but a clear correlation between Fe department and PGM department is observed.

No such simple correlation could be applied for Cu. The experimental data for Cu department versus the degree of Fe removal is shown in Figure 8.

The poor correlation for Cu is likely to be related to the fact that the γ value for Cu is not independent of composition, as found by Grimsey³. The experimental data showed that the ratio of the activity coefficients for Co and Ni was not a strong function of composition in this operating regime, while for Cu this aspect requires further evaluation.

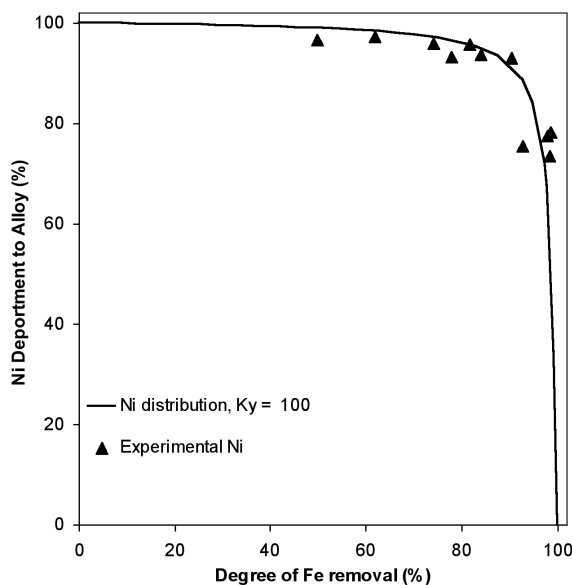


Figure 6. Correlation between the degree of Fe removal and Ni department to the alloy

Grimsey³ evaluated the behaviour of Cu during nickel matte converting operations and concluded that the behaviour of Cu appeared to be highly dependent on Fe concentration. Following Grimsey, the authors evaluated the $K\gamma$ relationship for Cu with respect to Fe concentration in the slag and alloy phases. Again, as per Equation [1] for Co and Ni, the interchange between Cu and Fe can be simplistically described by the following reaction between the liquid slag and alloy:



From this, the $K\gamma$ relationship was derived (as per Equations [2], [3] and [4]):

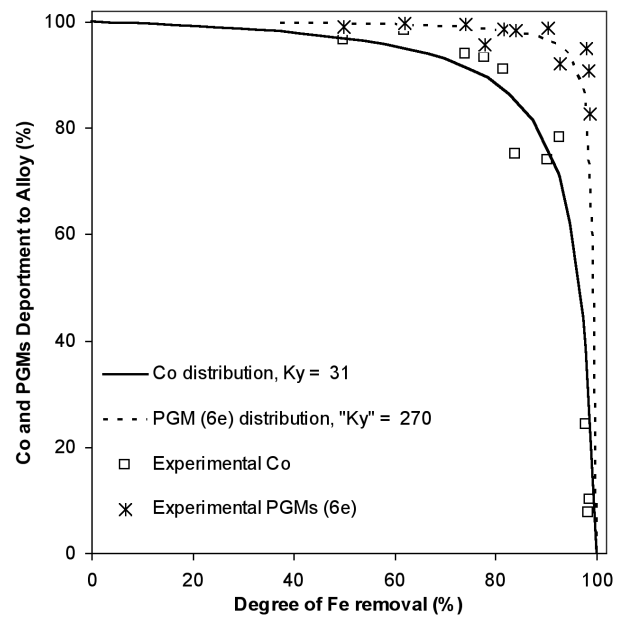


Figure 7. Correlation between the degree of Fe removal with Co and PGM department to the alloy

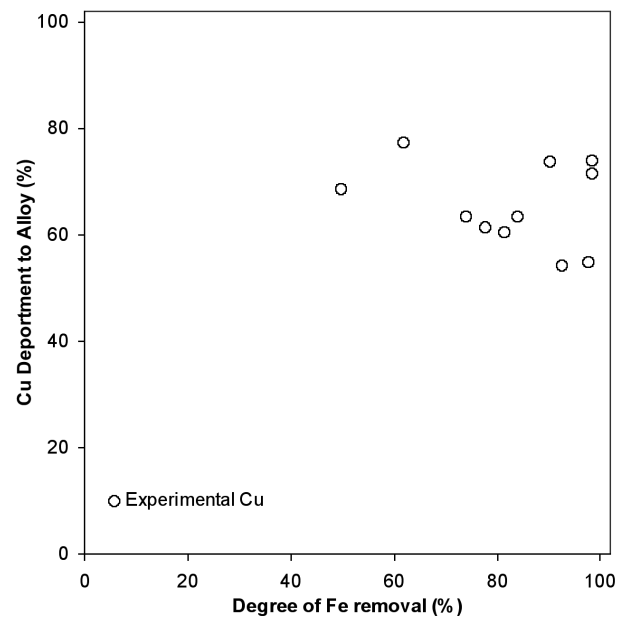


Figure 8. Experimental data for Fe removal and department of Cu to the alloy

$$K\gamma = \frac{x_{Cu} \cdot x_{FeO}}{x_{CuO} \cdot x_{Fe}} \quad [7]$$

Expressed in terms of numbers of moles:

$$K\gamma = \frac{n_{Cu} \cdot n_{FeO}}{n_{CuO} \cdot n_{Fe}} \quad [8]$$

The above equation may now also be expressed in terms of mass percentages, simply by taking into account a conversion factor to allow for the ratios of the molecular masses.

$$K\gamma = 0.973 \cdot \left(\frac{\%Cu \cdot \%FeO}{\%CuO \cdot \%Fe} \right) \quad [9]$$

A $K\gamma$ value for each test was calculated applying Equation [9], and these results are plotted in Figure 9. A clear empirical correlation was derived based on the Fe concentration in alloy as well as the recovery of Fe to the alloy (Figure 10).

The functional relationship shown in Figure 10, together with an equation of the form of Equation [5], allows one to express Cu recovery in terms of Fe recovery. However, because the relationship is so dependent on composition, care should be taken not to extrapolate this too far.

S behaviour during converting

The change in S concentration of the alloy during converting is shown in Figure 11. For the CaO-bearing slags used, only a minor decrease in the S concentration is initially observed during converting, and at 80% alloy mass loss, the S concentration is similar to that of the starting alloy. Given the large mass loss, a significant degree of S removal must be achieved to account for this. Recovery calculations indeed indicate 80 to 90% S removal for alloy with above 80% Fe removal (Figure 12). Alloys converted to more than 90% Fe removal typically contain 6 to 10% S. In contrast, converting to a similar degree of Fe removal using a CaO-free slag results in an alloy containing as much as 20% S. The variation in S removal as a result of the slag composition is not surprising, given that CaO-based slags are known for their high S capacity and are employed to desulphurize steel and other ferro-alloys to good effect.

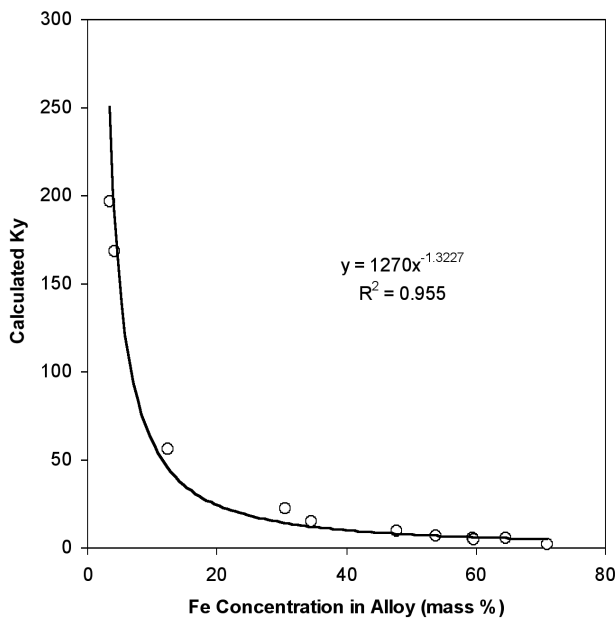


Figure 9. Correlation between $K\gamma_{Cu}$ and Fe concentration in alloy

The dependence of S removal on slag composition was also investigated at a larger scale using a Top Blown Rotary Converter (TBRC). This larger vessel (20 litres) had the advantage over alumina crucibles in that it was lined with a magnesia-chrome castable refractory. This enabled the use of the more traditional approach of fluxing the FeO-rich slag with SiO_2 to form a fayalitic slag. Heating and conversion of 20 kg alloy charges was carried out using a 120 kW water-cooled oxygen/propane lance. The resulting alloys (some of which are S-rich and could be classified as mattes) and slag compositions are shown in Tables V and VI respectively. (Note that the Si content of the alloy is likely to be from slag contamination of the sample rather than being present as Si itself.) Comparison of the alloy compositions during converting using CaO-free slags to those in which CaO was a component of the slag (Figure 13) indicate a distinct difference in the behaviour of S during converting. It is clear that CaO-bearing slags promote S-removal from the alloy during converting. Furthermore, the use of CaO-free fayalitic slags (approximately $2FeO \cdot SiO_2$), ultimately sees the production of a converted alloy (or matte as the case may be) similar in composition in terms of S concentration to that of typical converter matte produced by the South African PGM

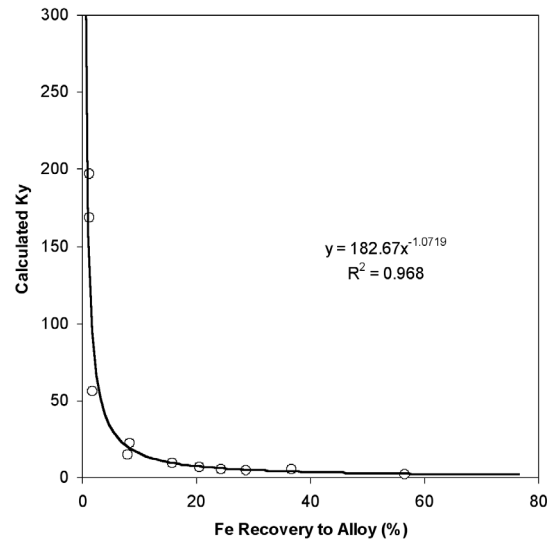


Figure 10. Correlation between $K\gamma_{Cu}$ and Fe recovery to alloy

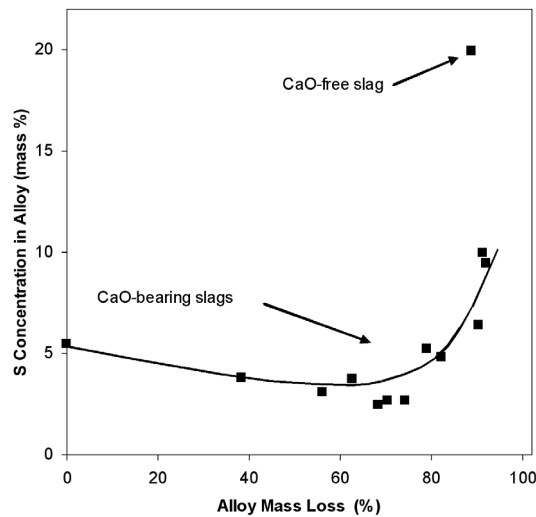


Figure 11. Concentration of S in the alloy as a function of alloy mass loss

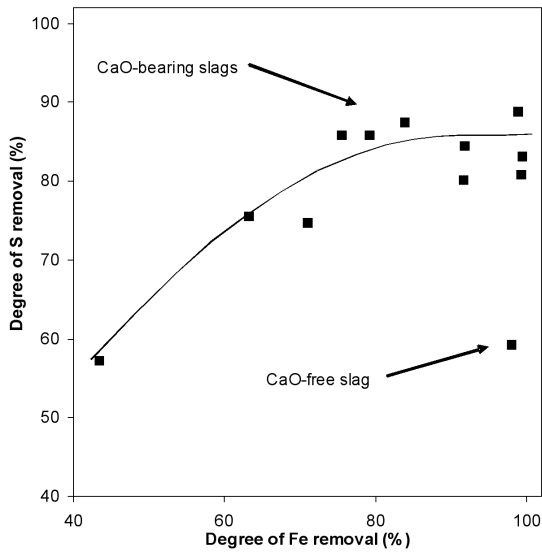


Figure 12. Comparison of the degree of S removal to Fe removal

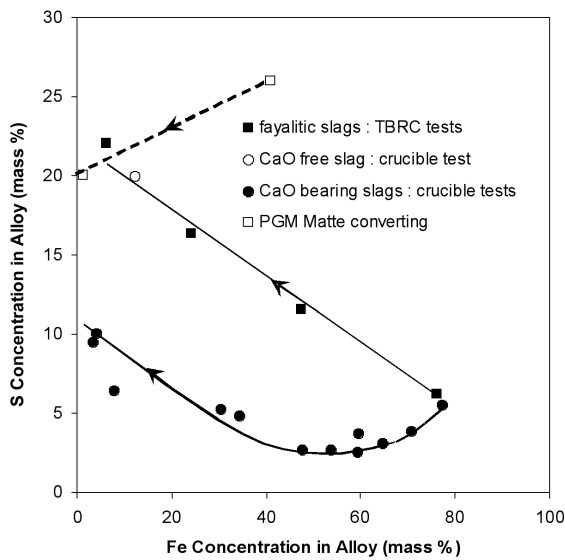


Figure 13. Comparison of the S and Fe concentration in alloys produced using CaO-based and CaO-free slags. Arrows indicate the direction in which alloy composition changes during converting. For comparison, the change in composition of typical PGM furnace matte⁴ during converting is also shown

industry. The relationship between S concentration and Fe concentration in the alloy is shown in Figure 13. It should be noted that the S concentration of the final converted product would depend on the concentration of S in the starting alloy and the ratio of S to other base metals in this alloy.

Large-scale converting

The laboratory-scale and pilot-scale converting work reported above was all based on converting as a batch process. However, there are good reasons for considering a continuous process for larger-scale converting work. A continuous reactor would be preferred to a batch reactor, as this is easier to schedule and operate, and this will also provide a single alloy composition instead of one that changes during the course of the converting operation. A batch process could see the composition of the melt change from a high-iron alloy to that of a matte, over the duration of the converting cycle. However, a continuous process would operate with a steady composition, i.e. that of the final product. Having to contain molten material of a single composition would prolong the life of the refractory lining of the vessel, in comparison with having to deal with an ever-changing composition.

A stationary non-tilting vessel is envisaged for the continuous converter. This is a mechanically simple option, which is expected to be more robust and reliable than having to operate a high-temperature device with moving parts. The converter should have separate tap-holes, at different elevations, for removing the slag and the converted alloy. Slag will be tapped more often than the converted alloy.

A top-blown vessel is envisaged. A number of lance designs are available for use. The non-consumable Siros melt lance, as used in Ausmelt and Isasmelt furnaces, is among the most industrially proven designs. Praxair's Coherent Jet oxygen lance has been used successfully in copper furnaces and steel-making furnaces. Another possibility would be to use an oxy-propane gas jet, as is used in Mintek's existing TBRC; or the lance design from the Kaldo furnace could be used. As a simple alternative, even a scaled-up version of the lab-scale oxygen delivery system could be used, namely a consumable hollow alumina tube immersed in the melt.

Given that the oxidation of iron is highly exothermic, it will be possible to supply the converter with a feed of solid granulated alloy. This will effectively decouple the operation of the smelting furnace from that of the converter,

Table VI
Chemical composition of the converted alloys produced using a TBRC (mass%)

| | Fe | Co | Ni | Cu | S | Si | Cr | Total |
|-------|------|------|------|------|------|------|------|-------|
| Start | 76.2 | 1.24 | 10.2 | 2.93 | 6.20 | 0.09 | 0.11 | 97.0 |
| 1T | 47.6 | 2.20 | 21.5 | 7.00 | 11.5 | 3.43 | 0.13 | 93.4 |
| 2T | 24.3 | 3.40 | 43.3 | 12.0 | 16.3 | 1.05 | 0.04 | 100.4 |
| 3T | 6.20 | 0.94 | 48.7 | 21.5 | 22.0 | 4.74 | 0.03 | 104.1 |

Table VII
Chemical composition of the slags produced using a TBRC (mass%)

| Test | MgO | Al ₂ O ₃ | SiO ₂ | CaO | Cr ₂ O ₃ | FeO | Total |
|------|------|--------------------------------|------------------|------|--------------------------------|------|-------|
| 1T | 0.83 | 0.34 | 35.5 | 0.15 | 0.69 | 59.7 | 97.2 |
| 2T | 1.64 | 0.33 | 21.7 | 0.70 | 0.31 | 72.3 | 96.3 |
| 3T | 1.58 | 0.52 | 22.6 | 0.08 | 0.57 | 69.3 | 94.7 |

and will allow a stockpile of material to be used as a buffer to ensure steady operation of the converter. An energy-balance calculation over the converter shows that it will be possible to control the temperature of the converter by using a mix of air and oxygen-enriched air. The solid alloy can also act as something of a coolant for the very exothermic iron oxidation reaction.

The following example reactions (with molar quantities listed in the reactions) illustrate that a thermal balance can be found somewhere between blowing with air and blowing with oxygen. Some oxygen enrichment is required with solid alloy feed.

Oxidation of iron with pure oxygen (reactants at 25°C, products at 1 500°C):

$\text{Fe} + \frac{1}{2}\text{O}_2 + \text{SiO}_2 \rightarrow \text{FeO}(\ell) + \text{SiO}_2(\ell)$ -1.10 kWh/kg Fe (exothermic)

Oxidation of iron with air (reactants at 25°C, products at 1 500°C):

$\text{Fe} + \frac{1}{2}\text{O}_2 + 1.88\text{N}_2 + \text{SiO}_2 \rightarrow \text{FeO}(\ell) + \text{SiO}_2(\ell) + 1.88 \text{N}_2$ +0.18 kWh/kg Fe (endothermic)

Melting of alloy constituents from solid at 25°C to liquid at 1 500°C:

| | |
|--------------------------|----------------------|
| Fe → Fe(ℓ) | 0.355 kWh/kg |
| Ni → Ni(ℓ) | 0.315 kWh/kg |
| Cu → Cu(ℓ) | 0.243 kWh/kg |
| Co → Co(ℓ) | 0.331 kWh/kg |
| Sulphides → Sulphides(ℓ) | 0.3 kWh/kg (typical) |

In the process of removing most of the iron from the alloy, it is expected that some of the valuable metals will report to the converter slag. However, these metals would not be lost to the overall process, as the intention would be to recycle the converter slag to the smelting furnace.

We know from previous experience that we can operate with the molten alloy at about 1 450 to 1 500°C, so we need a slag with a liquidus temperature that is compatible with this. For example, a slag comprising 57% FeO and 43% SiO₂ has a liquidus temperature of about 1 450°C. This requires an addition of SiO₂ that is almost exactly equal to the mass of Fe that is to be converted.

The preliminary conceptual outline of a continuous alloy converter presented here is expected to provide a sound basis for further large-scale alloy-converting work in the future.

Conclusions

Significant Fe removal has been demonstrated in a liquid-state oxygen converting process at laboratory scale.

Fe removal to the slag is favoured above that of Co and Ni, especially under less oxidizing conditions. Under more oxidizing conditions (approximately 80% Fe removal), the loss of Co, Ni, and, to a lesser extent, PGMs become significant.

The deportment behaviour of Co, Ni, and PGMs was evaluated and it was found that a simple equation could describe the relationship between the recovery of these elements as a function of the degree of Fe removal from the alloy. A single empirical K_γ value for each correlation could be applied to the experimental data. The empirical relationships for these elements can be used to predict the deportment of these elements to the slag phase and can assist in the selection of an optimum degree of Fe removal.

The behaviour of Cu under these conditions did not fit the correlation, indicating that K_γ for Cu is not independent of composition. An empirical correlation for K_γ as a function of Fe concentration in the alloy, as well as Fe recovery to the alloy, was established for Cu.

There appears to be an ability to change the distribution of S between the alloy, slag, and gas phases by changing the CaO content of the slag.

A preliminary conceptual outline of a continuous alloy converter that has been presented here is expected to provide a sound basis for further large-scale alloy-converting work in the future.

Acknowledgements

This paper is published by permission of Mintek and Braemore Platinum Smelters (Pty) Ltd. The authors would like to thank K. Ehlers for his assistance with the TBRC testwork.

References

1. JONES, R.T., DENTON, G.M., REYNOLDS, Q.G., PARKER, J.A.L., and VAN TONDER, G.J.J. Recovery of cobalt from slag in a DC arc furnace at Chambishi, Zambia, *SAIMM Journal*, vol. 102, Number 1, January/February 2002, pp. 5–9.
2. REINECKE, (nee GELDENHUYS), I.J. and LAGENDIJK, H. A twin-cathode DC arc smelting test at Mintek to demonstrate the feasibility of smelting FeNi from calcine prepared from siliceous laterite ores from Kazakhstan for Oriël Resources plc, *Infacon XI*, 2007, pp. 781–797.
3. GRIMSEY, E.J. Metal recovery in nickel smelting and converting operations, Extractive metallurgy of copper, nickel and cobalt, *Proceedings of the Paul E. Queneau International Symposium*, 21–25 February 1993, Warrendale, Penn.: The Minerals, Metals and Materials Society, 1993. vol. I, pp. 1 239–1 251.
4. JONES, R.T., *Platinum Smelting in South Africa*, *South African Journal of Science*, 95, November/December 1999, pp. 525–534.



Steven David McCullough

Chief Technician, Mintek

Joined MINTEK in 1986 where I spent 4 years studying Economic Geology at the Witwatersrand Technikon obtaining a national higher diploma. During my employment with MINTEK I was initially employed in the Thermo-chemistry section of Mineralogy which ultimately became the High Temperature Technology Division. My professional interests revolve around Pyrometallurgy and my association with MINTEK has allowed me a wide exposure to many high temperature processes including light metals, base metals ferro alloys and particularly precious metals.